# N O T I C E

THIS DOCUMENT HAS BEEN REPRODUCED FROM
MICROFICHE. ALTHOUGH IT IS RECOGNIZED THAT
CERTAIN PORTIONS ARE ILLEGIBLE, IT IS BEING RELEASED
IN THE INTEREST OF MAKING AVAILABLE AS MUCH
INFORMATION AS POSSIBLE

# Tuskegee Institute

## SCHOOL OF ENGINEERING

TUSKEGEE INSTITUTE
ALABAMA, 36088

DEPARTMENT OF ELECTRICAL ENGINEERING

TEL: 205-727-8200

NASA MARSHALL SPACE FLIGHT CENTER
RESEARCH GRANT NO NSG 8038
FINAL TECHNICAL REPORT

## MEASUREMENT OF LOSS ANGLE, VOLUME RESISTIVITY AND SURFACE RESISTIVITY OF INSULATING MATERIALS USED ON SOLAR CELLS

SUBMITTED BY

C. V. Doreswamy
Professor of EE
School of Engineering
Tuskegee Institute
Tuskegee Institute, AL   36088

APRIL 1980

## ABSTRACT

This report describes the complete measuring and test system developed at the Tuskegee Institute to measure the quality and the stability of insulating materials used on Solar Cell arrays for space applications.

The test set up and measurements are primarily aimed at the measurement and analysis of the degradation of the electrical insulating properties of material used on Solar Cells. Degradation characteristics of the material subject to thermal cycling, space plasma and very high electrical fields individually and in combination can be investigated. Ultimate breakdown tests can be conducted using ASTM Standard Methods D149.

# INTRODUCTION

The study of space plasma interaction with Solar Cell Arrays has been made by NASA and several other research centers. Test Samples consisting of photovoltaic materials – Silicon, Gallium Arsenide and dielectric materials – Kapton, Epoxy, Microsheet glass and Teflon were subjected to electron and proton bombardment and simulated plasma. The results of these investigations are available through published reports and literature [1, 2 .. 14]. From these investigations it was found that the dielectric materials of Solar Cell Array on an orbiting space craft in a charged particle environment (Space Plasma) is subject to several degradation processes.

The degradation process of the Insulating Material takes place in the following sequence.

1.  In an Solar Cell Array each interconnector and location will have a definite potential, depending on the total output voltage of the Solar Array, number of cells in series and parallel and other electric parameters.

2.  At some location on the array the generated voltage will be equal to the Space Plasma potential (7).

3.  The parts of the array which are below space plasma potential will repel electrons and parts above space plasma potential attract electrons and repel positive ions.

4. The attracted charged particles will collect on the insulated surface of the array.

5. If the dielectric material has a pinhole due a manufacturing defect or develops a pinhole due to thermal cycling, micro-meteoroid, UV radiation etc., all the charge collected on the insulator will be funneled through the pinhole causing high transient localized current. This transient current leads to arcing, "hot spots" and insulation destruction due to thermal effects. [5,6]

6. This pinhole effect is very severe with negatively biased electrodes. Arcing has been observed at voltages as low as -400v. This severe arcing is due to the fact that negatively biased electrodes emmit electrons thus contributing to higher electron currents. Higher temperatures caused by arcing and hot spots are likely to aggravate the condition. Higher electron currents due to thermionic emission are possible.

In general studies conducted indicate that

(a) It is a near certainty that the High Voltage Solar Cell Arrays operating at voltages over 2000v, will eventually develop pinholes due to thermal cycling. micrometeoroids and other causes which will allow plasma current collection.

(b) Hot Spots and arcing due to plasma collection and pinhole effects will eventually damage the insulation.

3

(c)  There is evidence of extensive damage of the insulating
     surface due to tracking and arcing.

(d)  The surface resistivity of Kapton decreases in the
     presence of charges by as much as a factor of 3000. [5]

The investigation of the dielectric properties is essential in view
of the strong evidence indicating plasma interaction can cause severe damage
to the insulating materials due to transient arcing and tracking. [5,6...]

A research project was started to investigate throughly the effects
of temperature cycling, very high Electrical fields and plasma interacting
in combination with the insulating materials.  This report discusses in detail
a test set up developed for such an investigation.  The report also describes
to theoretical basis of the instrumentation and Test Methods and their
Capabilities.  Detailed investigation will be carried out with various types
of insulating materials during the next phase of the project.

# PROPERTIES OF INSULATING MATERIALS

Insulating materials, which are also known as dielectric materials isolate components of electrical system from one another and from ground. They also provide Mechanical support for the components.

Three important parameters are used to indicate the quality and stability of the insulating materials. They are;

1.  Amount of heat loss produced in the materials when subjected to alternating electrical fields. The measurement and analysis of mechanisms of loss production, enables us to deduce the dynamics of molecular interactions and the structural changes in the material. The dissipation factor of the material characterizes the heat loss produced.

2.  Dielectric breakdown and breakdown strength of the material . The dielectric breakdown tests are destructive tests and intended for use as a control and acceptance tests. These tests are also used to ascertain the changes in the materials due to specific deteriorating causes.

3.  Surface and volume resistivity (Conductivity) characteristics. Surface resistivity and volume resistivity can be used to predict the low frequency dielectric breakdown and dissipation factor properties of some dielectric materials. These measurements are useful only if correlation can be established by supporting theoretical and experimental investigations.

To evaluate and experimentally investigate the changes in the quality and stability of the insulating macerials all the three above mentioned quantities must be measured. The changes in the dissipation factor, dielectric strength, surface resistivity and volume resistivity must be correlated with the variation of temperature, voltage and corona intensity.

The test set up developed to subject the test samples to the effects of temperature cycling , corona and high electrical voltages is described in the succeeding sections of this report. Test methods and instrumentation to measure loss angle, volume and surface resistivity, are discussed in the next section of this report.

6

# MEASUREMENT OF LOSS ANGLE OF INSULATING MATERIALS

The behavior of a dielectric in an alternating electrical field can be represented by means a Complex dielectric constant.

$$\varepsilon = \varepsilon' - j \varepsilon''$$

The dielectric can be schematically represented by a combination of a perfect capacitor and a resistance as shown in Fig (1). Only a perfect vacuum is a perfect dielectric and can be represented by a capacitor alone.

The power dissipated in the Capacitor due to dielectric losses is given by
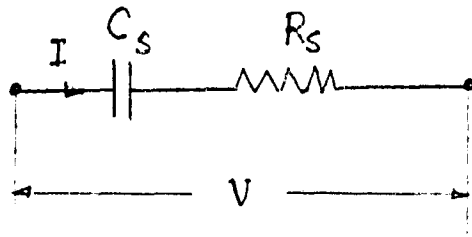
$$P = V^2 \omega c \tan\delta.$$

$\tan\delta$ is called the dissipation factor of the dielectric and $\delta$ is known as the loss angle of the dielectric. Fig. 1 (c) shows the phasor diagram defining the angle $\delta$.
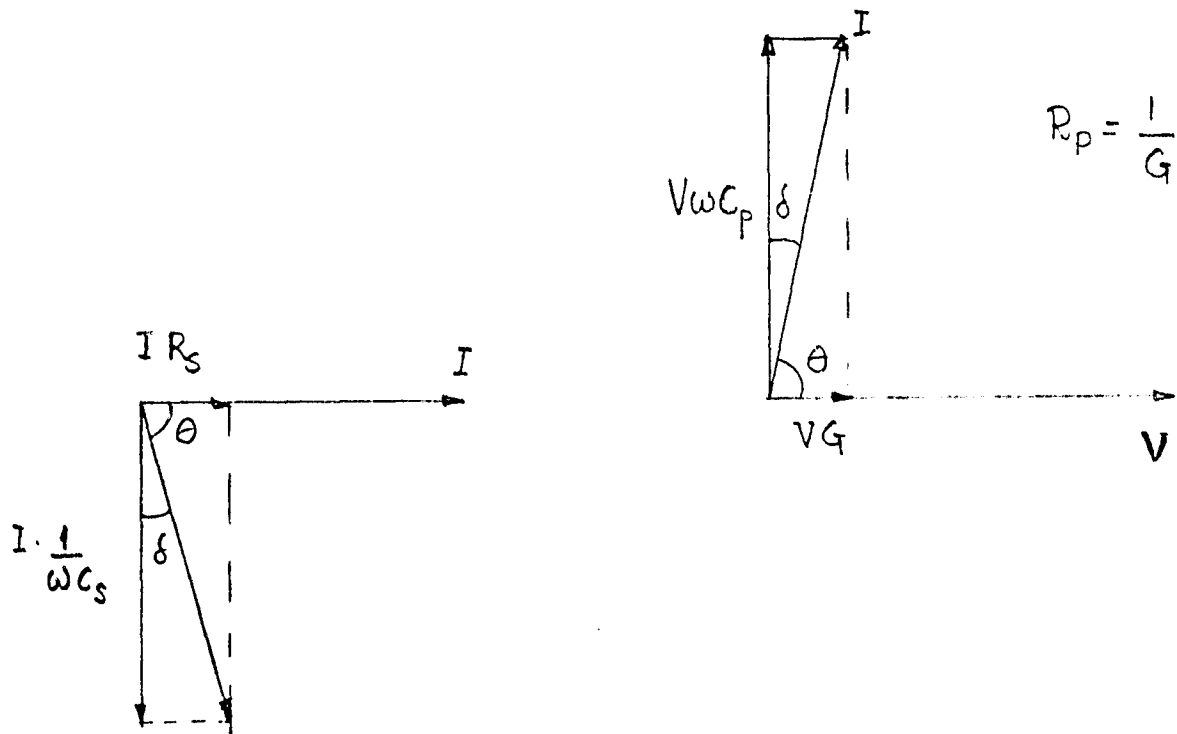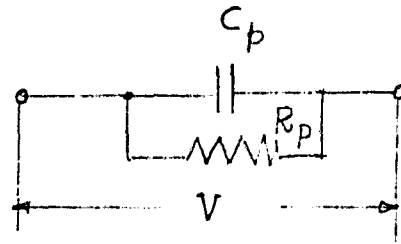
It can be shown that

$$\tan\delta = \frac{\varepsilon''}{\varepsilon'}$$

The dielectric losses in the insulating materials are caused by, various polarization mechnisms that occur inside the material when an electrical field is applied. In general both $\varepsilon'$ and $\varepsilon''$ are dependent upon temperature, frequency,

7

Series Circuit                    Parallel Circuit

$C_S$   $R_S$                      $C_p$

$I$                                $R_p$

$V$                               $V$

$R_p = \dfrac{1}{G}$

$I R_S$        $I$        $Vω C_p$   $δ$   $I$

$θ$                        $θ$

$I \cdot \dfrac{1}{ωC_S}$   $δ$     $VG$        $V$

Phasordiagrams

Fig (1) Equivalent Circuit of a Lossy Capacitor.

and applied electrical field. The measurement of the variation of the value of tanδ, with voltage, temperature and frequency enables one to deduce the dynamics of molecular interactions. The value of the dissipation factor is a measure of the heat generated in the material and must be held small. Dissipation factor is used indicate the quality of the insulating material with other correlating data characterizing the insulating material.

Dielectric loss index is defined as

$$K'' = \varepsilon \ \tan\delta$$

## METHODS OF MEASUREMENT OF THE DISSIPATION FACTOR OF THE INSULATING MATERIALS

Methods for measuring capacitance and tanδ can be classified into three groups: Bridge methods, resonance methods and deflection methods. The choice of the measurement system is dependent on the frequency and accuracy required. The deflection method is a direct method where the voltage, current and the power loss are measured by conventional meters and employed only at power line frequencies of 25 to 60 Hz and at high voltages, and is not very accurate.

Null methods are most commonly used in measuring a. c. loss at high voltages. The resistive or inductive ratio arm capacitance bridge in its various forms can be used over the frequency range from less than 1 HZ to several MHZ. The lowest loss tangents to be mueasured require a sensitivity of $10^{-6}$ rad. This limits the choice of methods and calls for considerable care.

## SCHERING BRIDGE

Keeping in view all the requirements regarding the accuracy and opperating stresses on the insulating material, it was decided to use the high voltage Schering Bridge for the measurement of tanδ in this investigation.

Schering bridge was suggested in 1920 by Schering as a method for measuring dielectric losses at high voltages. The bridge proves to have many advantages and to be versatile. The enormous development in high voltage technology has resulted in a very wide use of the method for tests of the losses in cables and in insulators at high working voltages. Moreover the bridge is also one of the best ways for testing small condensers at low voltages with very high precision.

Referring to Fig. (2) $C_x$ is the effective capacitance $R_x$ the equivalent series loss resistance of the sample condenser $C_x$. $C_s$ is a standard capacitor, $C_1$ is a variable condenser. $R_1$ and $R_2$ are non-reactive resistances.
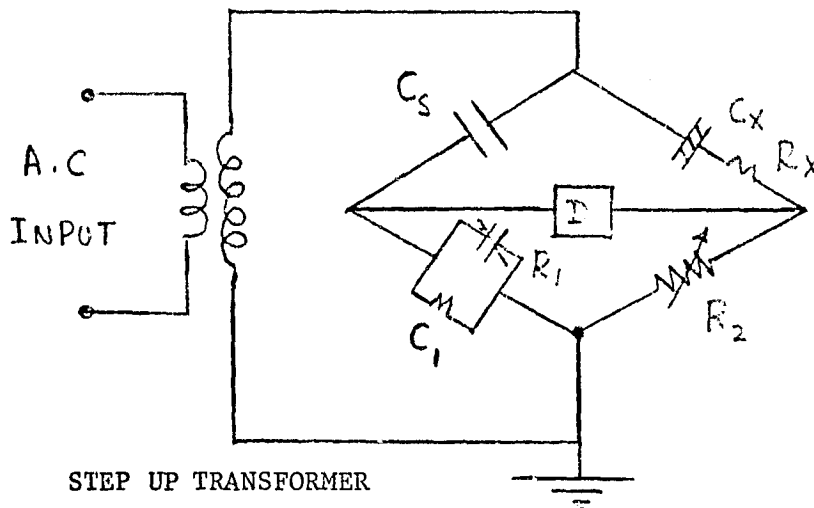


Fig (2) High Voltage ScheringBridge

Writing down branch impedances

$$Z_1 = \frac{1}{j\omega C_S}$$

$$Z_3 = \frac{1}{1/R_1 + j\omega C_1}$$

$$Z_2 = R_X + \frac{1}{j\omega C_X}$$

$$Z_4 = R_2$$

At balance we have

$$\frac{Z_1}{Z_3} = \frac{Z_2}{Z_4}$$

$$Z_2 = \frac{Z_1}{Z_3} Z_4$$

Hence

$$R_X + \frac{1}{j\omega C_X} = \frac{1}{j\omega C_S}\left(\frac{1}{R_1} + j\omega C_1\right) R_2$$

$$R_X + \frac{1}{j\omega C_X} = \frac{R_2}{j\omega C_S R_1} + \frac{C_1 R_2}{C_S}$$

Equating real and imaginery parts

$$R_X = \frac{C_1}{C_S} R_2 \quad \text{and} \quad C_X = \frac{R_1}{R_2} C_S$$

Loss angle $\tan\delta = \omega C_1 R_1$.

11

The Schering bridge is very safe to operate. The branches containing $C_1$ and $R_2$ have very little voltages across them since their impedances are very small in comparison with those of the condenser branches having $C_x$ and $C_s$. This fact makes Schering bridge useful for high voltage measurements. The voltage across $R_2$ may be one ten-thousandth of that applied to bridge. Hence the detector points are never more than a few volts above earth potential so the balancing circuit may be adjusted with perfect safety. As an additional safeguard, the low voltage portions of bridge, $R_2$, $R_1$ and $C_1$ are contained in an earthed metal enclosure, the switches effecting the necessary balancing adjustments being provided with insulated knobs.

The direct action of the electric field of high voltage electrodes of $C_x$ and $C_s$ upon the low voltage portions of the bridge, namely, the leads from low voltage electrodes of $C_x$ and $C_s$, detector and low voltage branches is extremely important and errors due to this cause can be avoided by the adoption of an appropriate system of electric shielding.
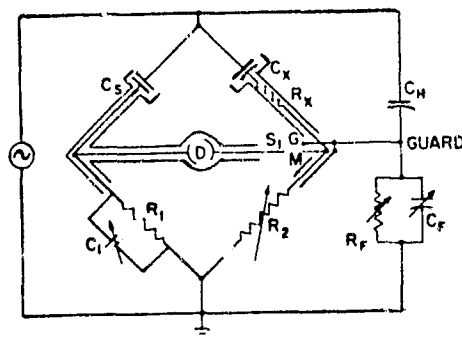


Equations

$$C_x = \frac{R_1}{R_2}\, C_2$$

$$\tan\delta = \omega C_1 R_1$$

Fig (3) Schering Bridge With Wagner Earth

Since the impedances of $C_x$ and $C_s$ are very high compared to $R_1$ and $R_2$, sensitivity of the bridge is considered low as the impedance of the branches deviate so far from the conditions of maximum sensitivity. However at high voltages and with a sensitive detector, the available sensitivity is adequate for all practical requirements. The sensitivity of this bridge is proportional to frequency.

The complete circuit consists of power supply, Schering Bridge, Wagner earth and detector. Schematic diagram of the Schering Bridge is given in Figure 2 and Figure 3 shows the shielding and Wagner Earth.

The wagner earth is used to bring the potential of the measuring electrode near to earth potential. Hence the pick up of spurious signals greatly reduced. It is required to obtain maximum detector sensitivity to the bridge component being balanced. Bridge balancing is achieved by varying $C_1$ and $R_2$ with switch $S_1$ in position M to obtain minimum deflection in detector D. After that, switch $S_1$ is shifted to position G and the same minimum deflection is obtained by varying $C_F$ and $R_F$ such that the detector shows no change in balance by switching $S_1$ to M or G. the loss tangent of the specimen is then directly proportional to capacitance $C_1$ and is given by

$$\tan \delta = \omega C_1 R_1$$

where $\omega$ = angular frequency, $R_1$ is of constant value and $C_1$ is the value at which balance is achieved. A low noise high gain tuned amplifier is used in the Null detector Stage to accurately detect the voltage unbalance. The operating frequency of the amplifier is determined by selective bandpass filters which can be tuned to 60 HZ, 50 HZ or 25 HZ corresponding the frequency of the test high voltage.

# SERIES AND PARALLEL EQUIVALENT CIRCUITS OF CAPACITOR WITH DIELECTRIC LOSSES

Fig 1 (a, b) show the equivalent circuits of a lossy capacitor and Fig 1 (c, d) show phasor diagrams corresponding to these equivalent circuits.

The dissipation factor of the parallel circuits is defined as

$$\tan \delta_P = \frac{I}{I_R/I_c} = \frac{1}{\omega C_P R_c}$$

and that of the series equivalent circuit

$$\tan \delta_s = \frac{V_R}{V_c} = R_s \omega c_s$$

In general a capacitor possesses both the series and parallel loss resistances as shown in fig (4). Depending on the frequency of the applied voltage only one of them dominates. In fig (4) $R_s$ represents resistance of the connecting leads, electrode contact resistances and the part of the dielectric loss whose characteristics can be more accurately described by a series equivalent circuit.
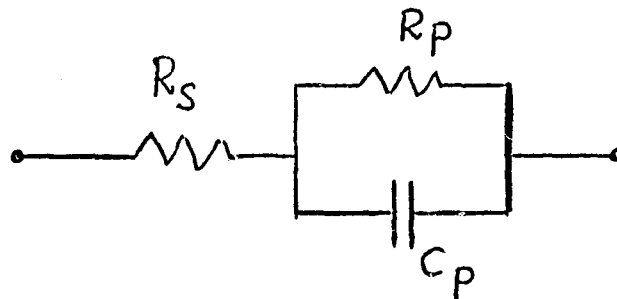


Fig. 4

14

Resistance $R_p$ represents a measure of the dielectric losses inside the material. At low frequencies $\frac{1}{\omega cp} \gg R_s$ and only parallel circuit is effective.

At high frequencies and above the measured lossed are determined by $R_s$. However at any particular frequency both the circuits are accurate. But over a wide frequency range either of the circuit alone is inaccurate.

The relation between series and parallel equivalent resistance and capacitances are given by,

$$R_p = R_S\left(1 + \frac{1}{\tan^2\delta}\right) \qquad C_p = \frac{C_S}{(1 + \tan^2\delta)}$$

$$R_S = \frac{R_p}{\left(1 + \frac{1}{\tan^2\delta}\right)} \qquad C_S = C_p(1 + \tan^2\delta)$$

The equivalent converted values are valid for only one frequency because the dissipation factor $\tan\delta$ itself is frequency dependent.

15

## Accuracy of The Bridge Measurements

## Loss Reference Standard Capacitor

The accuracy of the measurement of the small dissipation factors
are dependent on the constancy of the bridge elements and the error angles
of the particular elements.  The loss reference is the high voltage
Standard Capacitor.  The characteristics of this capacitor has a
direct influence on the accuracy of measurement.  The loss refeerence
is compressed gas (Carbon Dioxide) Standard Capacitor 100 pF, 190 Kv
rms. $\tan\delta \geq 10^{-5}$.  The Standard Capacitor used in his investigation
is an almost ideal capacitor.  It is worth mentioning here the capacitor
and bridge circuit elements used in this investigation are used in Standard
laboratories internationally.  Fig (7) shows the experimental set up with
standard capacitor and the test specimen inside the environmental chamber.

## DEPENDANCE OF DISSIPATION FACTOR (TANδ) AND LOSS INDEX ON VARIOUS FACTORS

The dielectric constant and the loss  angle of insulating materials
are not constant over the wide frequency range (D.C. to 3GHZ) the insulating
materials are used.  The changes in the dielectric constant are produced by
the changes in dielectric polarizations in the material.

Frequency Fig (5) shows a the variation of dielectric constant and loss
index with frequency.  The lowest value of dielectric constant accurs at
the highest frequency and is determined by electronic or atomic polarization.
Each polarization furnished a maximum and the frequency at which the maximum
value of loss index accurs is known as the relaxation frequency for that
polarization.

16

## VOLTAGE

All dielectric polarizations except the interfacial are nearly in-
dependent of the electrical field in the material. The value of tan$\delta$ is
practically a constant with the increase the electrical field until such a
value is reached that the ionization occurs in voids in the material or on
the surface. Any sudden increase in the value of tan$\delta$ invariably indicates
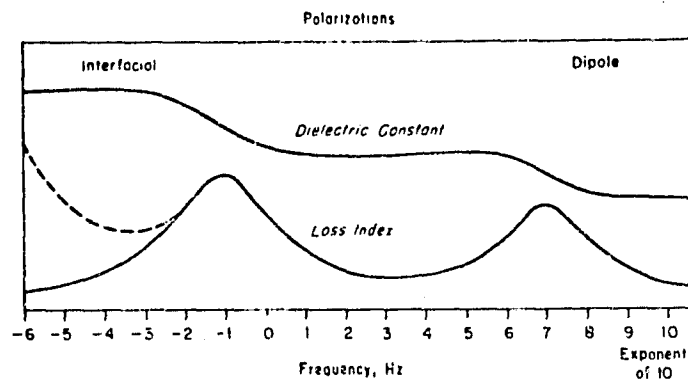a local breakdown of the material and will ultimately lead to total failure
of the insulation.



FIG (5) POLARIZATIONS [15]

## Temperature

The major effect of the temperature on an insulating material is to
increase the relaxation frequencies of its polarizations. At lower frequencies
where interfacial and dipole polarizations are effective, the temperature
coefficient of the dielectric constant is positive. The temperature co-
efficient of the dielectric constant is negative at high frequencies where
the electronic and atomic polarization effects are active.

17

The temperature coefficient of the dielectric loss index may be positive or negative depending on the relation of the measuring frequency to the relaxation frequency. It will be positive for frequencies higher than the relaxation frequency and negative for lower frequencies. At 60Hz, temperature coefficient of dielectric loss index is positive. The dissipation factor tan$\delta$ increases appreciably when the temperature increases.

# CHOICE OF ELECTRODES FOR MEASURING A. C. CAPACITANCE AND DISSIPATION FACTOR $\tan\delta$

## GENERAL CONSIDERATIONS

The measurement of $\tan\delta$, capacitance and complex dielectric constants are based upon measurements with the specimen of the material placed in an electrode system, whose vaccuum capacitance can be either accurately calculated or measured in the absence of the test specimen. Therefore the problem is mainly of determining two capacitance values accurately, either by calculation or indirectly by comparison with a capacitance standard whose capacitance is accurately known.

Fig 6 shows an electrode system consisting of two parallel plate electrodes, between which the unknown material is to be placed for measurement. In addition to desired inter electrode capacitance $C_v$ the system included also edge capacitance $C_e$, capacitance to ground of the outside face of electrode $C_g$, is independent of outside environment, all others being dependent upon proximity of other objects. It becomes necessary then to eliminate these undesired capacitances. If one measuring electrode is grounded, as is often the case, all capacitances except the ground capacitance of grounded electrode and its lead are in parallel with desired capacitance. If a guarded test cell is used, the capacitance to ground no longer appears and capacitance at terminals is $C_v$., $C_e$ and lead capacitance can be made very small.
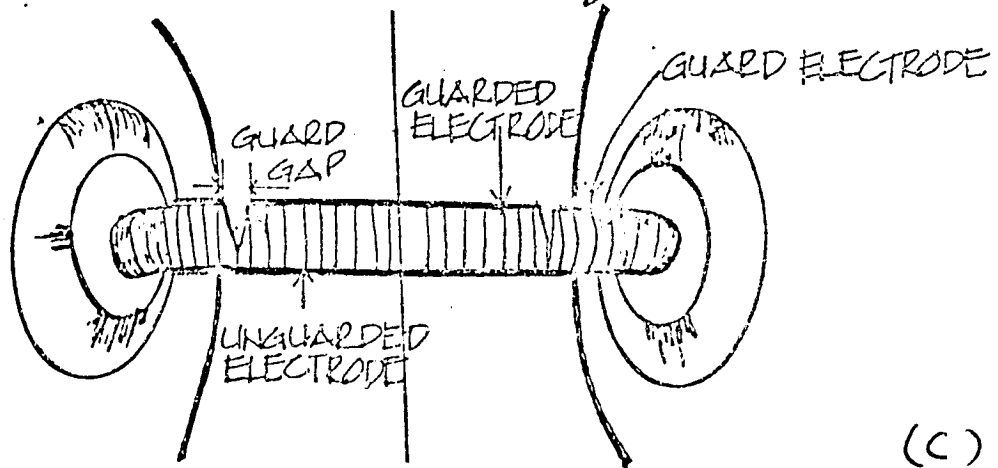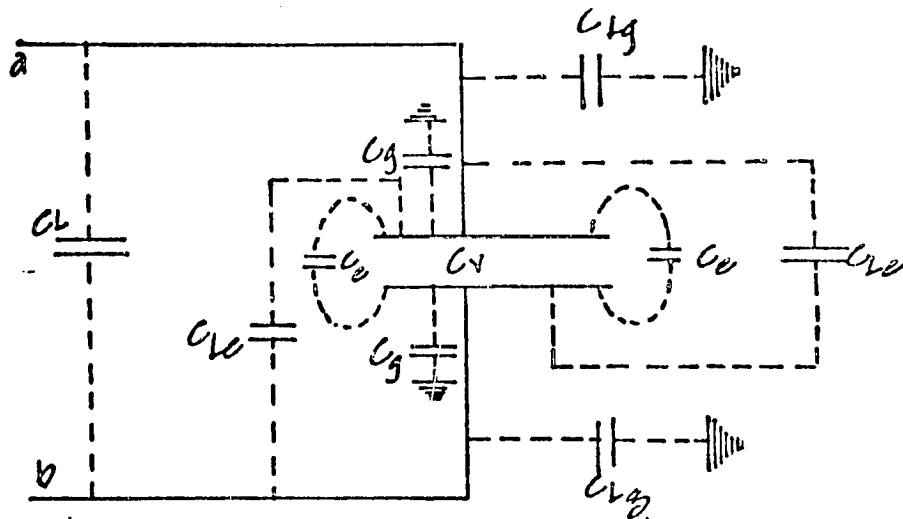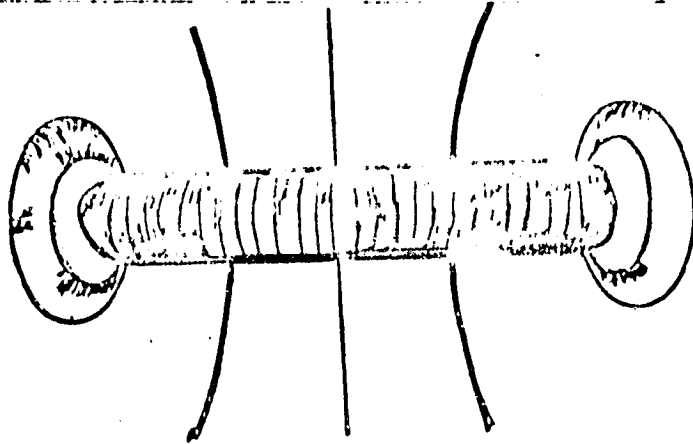
FLUX LINES BETWEEN ELECTRODES



(a)



(b)



(c)

FIG 6. GUARDED PARALLEL-PLATE ELECTRODE SYSTEM.

Edge capacitance can be calculated in air. In routine work where best accuracy is not required, it is convenient to use unshielded, two electrode system and make necessary corrections.
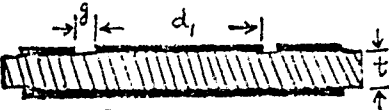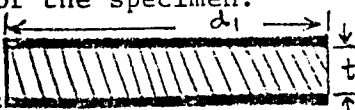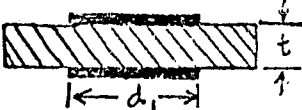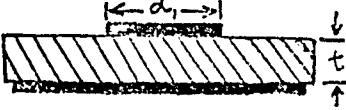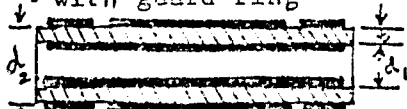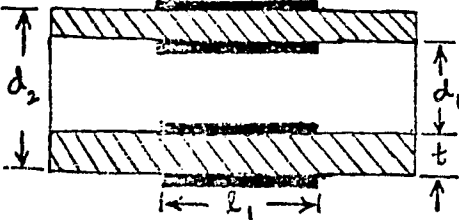
The fringing and stray capacitance at the edge of guarded electrode is practically eliminated by the addition of a guard electrode as shown in Fig. 6 (c). If the the test specimen and guard electrode extend beyond the guarded electrode by at least twice the thickness of the specimen and guard gap is very small, the field distribution in the guarded area will be identical with that existing when vacuum is dielectric and ratio of these two direct capacitances is the dielectric constant. Furthermore the field between the active electrodes is defined and the vacuum capacitance can be calculated with the accuracy, limited only by the accuracy with which the dimensions are known. Although the guard is commonly grounded, arrangement can be made to permit grounding either measuring electrode or none of the electrodes to accommodate the particular three terminal measuring systems being used. If the guard is connected to ground or to a guard terminal on the measuring circuit the measured capacitance is the direct capacitance between two measuring electrodes. If, however, one of the measuring electrodes is grounded, the capacitance to ground of ungrounded electrode and leads is in parallel with the desired direct capacitance. To eliminate this source of error, the ungrounded electrode should be surrounded by a shield connecting to guard.

<u>Micrometer Electrodes</u>:   Micrometer electrode system was developed   19
to eliminate the errors caused by series inductance and resistance of the
connecting leads of the measuring capacitor at high frequencies.   Fig 11
shows the micrometer electrode system proposed to be used for measurements
of tan$\delta$ at high frequencies.   Carefully calibrated the micrometer electrode
system eliminates the need for corrections for edge and ground capacitances.
This electrode system will be used for measurements at the frequency range
of 1 MHZ – 30 MHZ.

<u>Geometry of Specimens</u>:   The practical geometrical shapes of electrode
systems for which the capacitance can be most accurately calculated are
guarded flat parallel plate electrodes and coaxial cylinder electrodes.
The equations for calculating the interelectrode capacitances are listed
in Table I (ASTM).  Flat circular electrodes are generally used for testing
Solid Sheet insulating materials whereas coaxial cylinderical electrodes
are used for liquid dielectrics.  Corrections for stray field edge effects
and the effects of the guard gap are made according to the methods described
in references 15 and 16.  The effective area of the guarded electrode is
greater than its actual area by approximately half the area of the guarded
gap.   [16]

TABLE 1.—Calculation of Vacuum Capacitance and Edge Corrections

| Type of Electrode (dimensions in centimeters) | Direct Inter-Electrode Capacitance in Vacuum pb | Correction for Stray Field at an Edge, pF |
|---|---|---|
| (i) Disk electrodes with guard-ring  | $C_v = E'_o \dfrac{A}{t}$ <br><br> $= 0.088542 \dfrac{A}{t}$ <br> WHERE <br> $A = \dfrac{\pi}{4}(d_1 + B{*}g)^2$ | $C_e = 0$ |
| (ii) Disk electrodes without guard-ring. Diameter of the electrodes = diameter of the specimen.  | | where $a \ll t$ <br> $\dfrac{C_e}{P} = 0.029 - 0.058 \times \log t$ |
| (iii) Equal electrodes smaller than the specimen  | $C_v = .06954 \dfrac{d_1^2}{t}$ | $\dfrac{C_e}{P} = 0.019\, K_g' = 0.058 \log t \\ \qquad \div 0.01$ <br> where $K_g$ = an approximate value of the specimen dielectric constant, and $a \ll t$ |
| (iv) Unequal electrodes:  | | $\dfrac{C_e}{P} = 0.041\, K_g' - 0.077 \log t \\ \qquad\qquad + 0.045$ <br> where $K_g'$ = an approximate value of the specimen dielectric constant, and $a \ll t$ |
| (v) Cylindrical electrodes with guard-ring  | $C_v = \dfrac{0.24160(\ell_1 + B{*}g)}{\log \frac{d_2}{d_1}}$ | $C_e = 0$ |
| (vi) Cylindrical electrodes without guard-ring  | $C_v = \dfrac{0.24160\,\ell_1}{\log \frac{d_2}{d_1}}$ | If $\dfrac{t}{t-d_1} < \dfrac{1}{10}$ <br> $\dfrac{C_e}{2P} = 0.019\, K_g' - 0.058 \log t \\ \qquad\qquad\qquad + 0.010$ <br> $P = \pi(d_1 + t)$ <br> where $K_g'$ = an approximate value of the specimen dielectric constant |

B* See Reference 15 Page 55

<u>HIGH VOLTAGE TEST SPECIMEN HOLDER AND ELECTRODE</u>
<u>SYSTEM FOR MEASURING TAN? AT HIGH VOLTAGES</u>
<u>AND HIGH TEMPERATURES</u>

The high voltage electrode system was designed to measure the variation of tanδ, with the changes in temperature, Corona intensity and Electrical Voltages. This system shall be capable of performing satisfactorily in the temperature range of -100°F to + 450F and test high voltages up-to Kv r.m.s. 60 HZ.

For the purpose of this experiment, the three terminal method was selected. Guarded electrodes arrangement is considered to be quite an accurate method because it involves the least corrections. No edge capacitance or fringing and stray capacitance appears in the results. Ground capacitance is also made to zero. This type of arrangement is shown in Figure (7). When the guard gap is small, field distribution is very much the same as if the vacuum is dielectric; then the three terminal method becomes a referee method.

The electrode system consists of two circular disk type electrodes with a guarding ring electrode. The insulating material under investigation is placed between the electrodes as shown schematically in Fig (7).
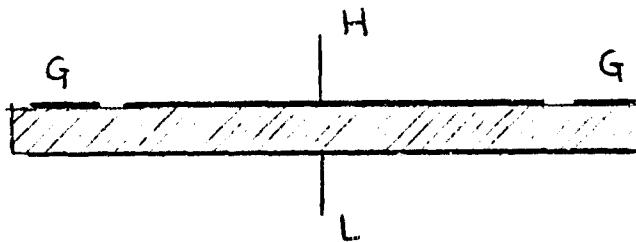


FIG 7 SCHEMATIC DIAGRAM OF GUARDED ELECTRODE

**Fig(8)**   Shows the details of the electrode System.

The heavy specimen holder consists of electrodes designed to lay cylindrical with the guard ring and guarded electrode in a co-axial arrangement. The cylindrical guard ring and guarded electrode are made of brass and they are separated by a cylindrical tube of teflon. The lower and upper surfaces of the ring and this electrode are ground to nearly optical flatness. A small hole is made in the outer periphery of the ring and teflon tube up to the inner measuring electrode and a co-axial cable is connected such that one of its wires connected measuring electrode to detector and the other connected ring to ground terminal. Teflon cylindrical sheet also maintains a uniform gap between measuring electrode and ring. High voltage electrode, which is below the measuring electrode, is also made of brass and machine ground to perfect flatness. This electrode rests on a cylinder of teflow with an aluminum base. The high voltage connector enters from the side of the teflon cylinder and is attached to the back surface of the high voltage electrode. The diameter of the high voltage electrode is made larger than the  ring. Fig (9) shows the photograph of the Electrode System.
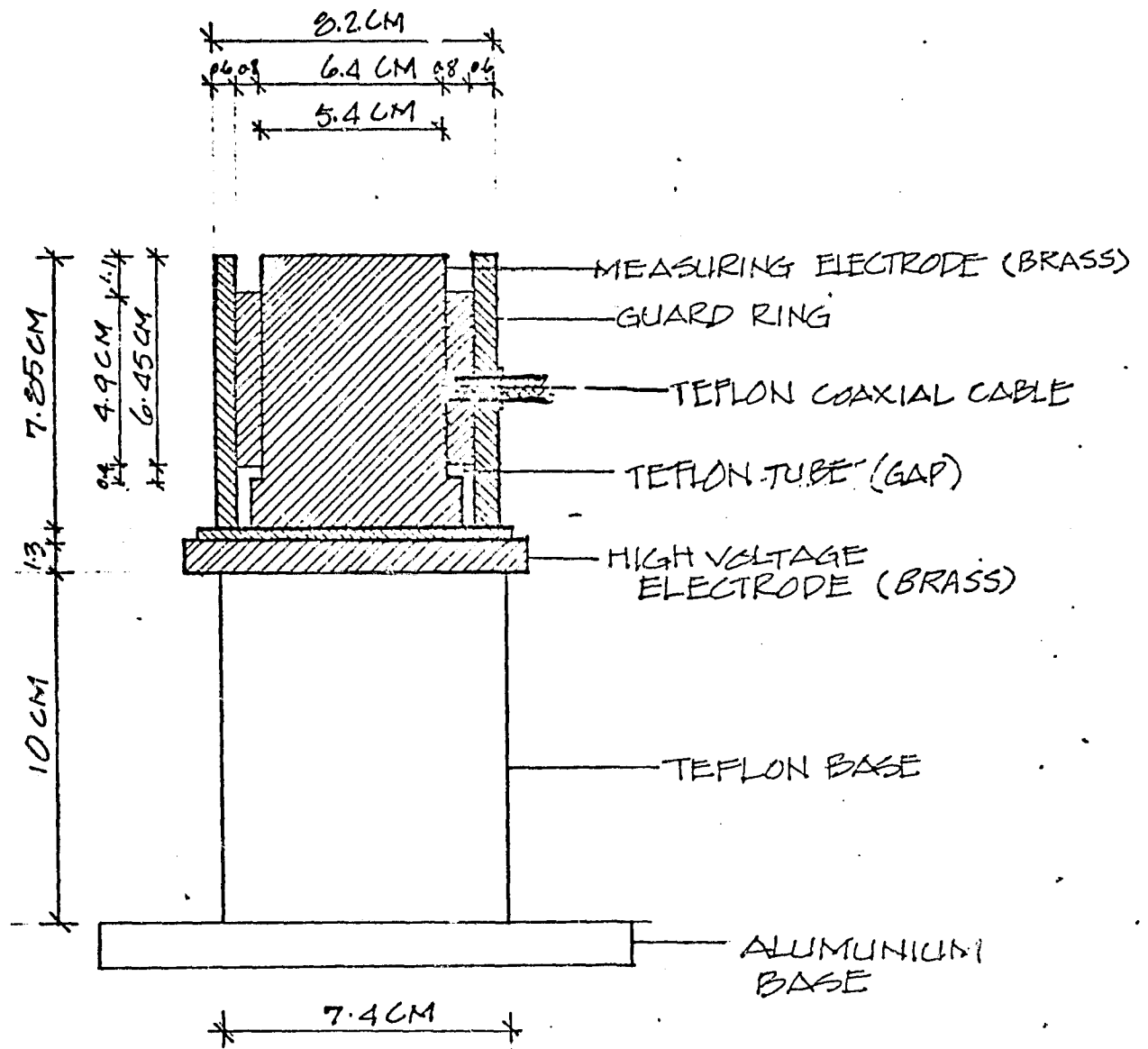
Dimensions shown on figure:
8.2 CM, 6.4 CM, 5.4 CM, 7.25 CM, 4.9 CM, 6.45 CM, 10 CM, 7.4 CM

- MEASURING ELECTRODE (BRASS)
- GUARD RING
- TEFLON COAXIAL CABLE
- TEFLON TUBE (GAP)
- HIGH VOLTAGE ELECTRODE (BRASS)
- TEFLON BASE
- ALUMINIUM BASE

FIG 8          SCREENED ELECTRODE SYSTEM FOR

HIGH VOLTAGE CAPACITANCE MEASUREMENTS

26

The whole assembly of the electrode system with a test specimen was put in the test chamber described earlier. High voltage was applied and gradually increased to 10Kv r.m.s.

Temperature inside the chamber was also varied from $- 75^{\circ}$ and $+ 400^{\circ}F$, the electrode system performed well. No flashovers or spurious discharges were observed. An the connections and the high voltage systems wage tested and found to be Corona free-up to 10 kv. r.m.s.

This complete system is now ready and calibrated for the measurement of tan$\delta$ and dielectric constants of sheet type insulating materials. The measurement of tan$\delta$ can be correlated both to the quality and stability of the insulating material under investigation.

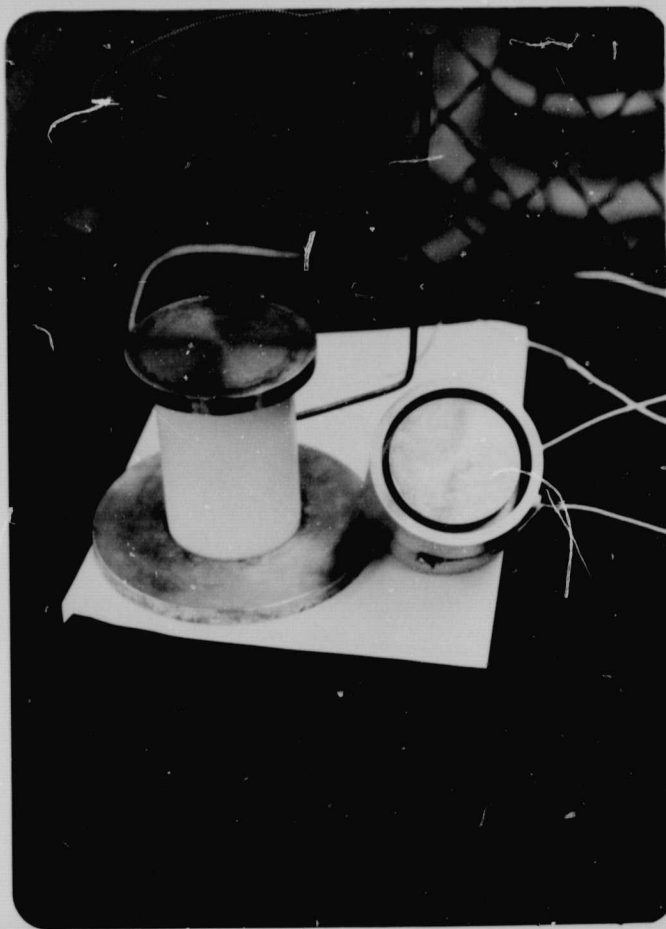**Fig 9.** Screened Electrode System for Measurement of tan δ and
Capacitance at High Voltages.

# MEASUREMENT OF TANδ AND CAPACITANCE AT HIGH FREQUENCIES

Measurements will also be made at high frequencies up-to 30 MHZ.
Resonance methods are used to measure both tanδ and capacitance. Fig (10)
shows the schematic diagram for the HP 4342A Q Meter used for these
measurements. A three terminal guarded micrometer electrode and a two
terminal micrometer electrode are used to test the dielectric materials.
Fig shows the guarded micrometer electrode. The capacitance standard on
the Q meter has calibration accuracy traceable to National Bureau of
Standards. The edge correction for the unguarded electrodes were applied
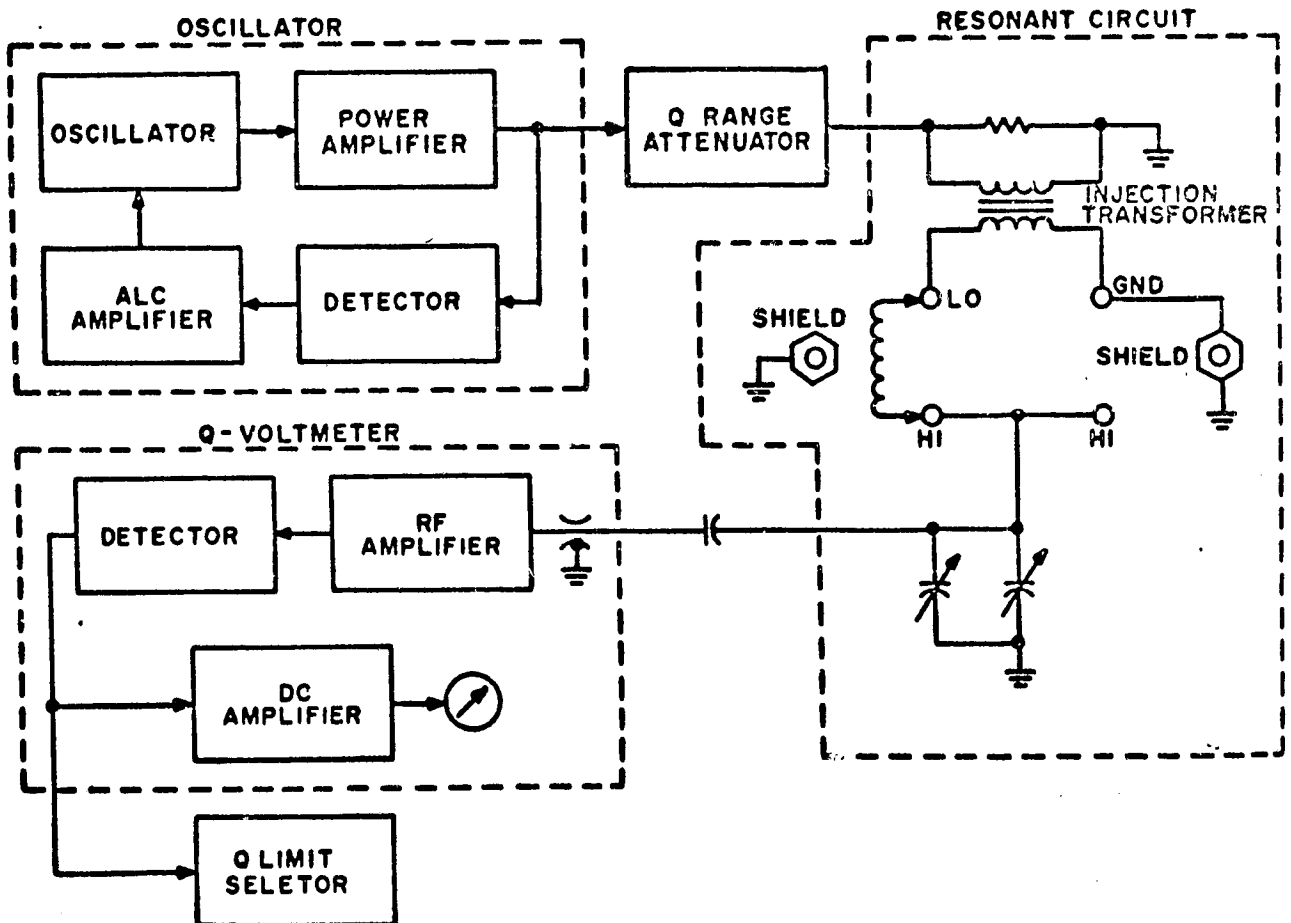according to ASTM Standards D150
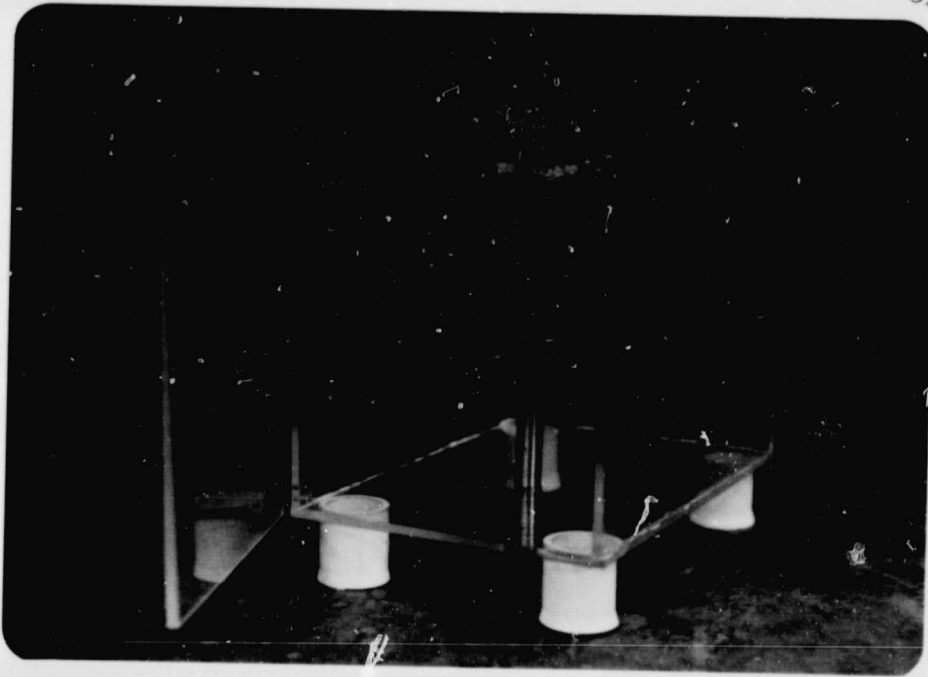


Fig. 10 Q. Meter Schematic Diagram

28

Fig 11.   Electrode System for Breakdown Tests



Fig 12.   Micrometer Electrodes and Dielectric Sample Holder for
Capacitance Measurements

## EXPERIMENTAL CHAMBER

In order to investigate the variation of the important parameters
that characterize the quality and stability of the insulating material,
it is very essential that a test chamber be engineered to satisfy the
following requirements.

a) It should be possible to subject the insulating materials
to thermal cycling between the operating temperatures of the
Solar Cell Array.

b) Provision must be made to inject corona and space charges
on to the surface of the insulating material under in-
vestigation at various temperatures.

c) It should be possible to conduct measurements of dis-
sipation factor and breakdown voltage, with the test
sample inside the chamber and at high voltages.

d) The test chamber and associated equipment must not
generate spurious signals or interferences which might
render the measurements inaccurate.

An environmental chamber which can accomplish the requirements
listed above has been constructed, with the following capabilities.

1. The chamber is capable of providing and maintaining and desired
test chamber temperature between the ranges of $-100^{O}F$ to $+450^{O}F$.

2. Provision has also been made apply test Highvoltage to the
material sample in the test conductor.

3.   Automatic temperature control devices and temperature measuring
     elements have been calibrated using standard methods of temperature
     measurement.

4.   As the test samples are of small physical dimensions, it will
     be assumed that the temperature at all points of the test sample
     is uniform and is indicated by the steady temperature of the test
     chamber.  Any introduction of thermocouples or transducers in the
     electrode system will distort both the thermal and electrical
     stress fields and hence is highly undesirable.

5.   It is essential that all the electrical supplies, connections
     and electrodes shall be corona free.  The application of electric
     voltages shall not introduce any extraneous free charges –
     electrons or positive ions – into the test sample.

6.   To make certain that the requirement listed in (5) above is
     satisfied, the test chamber with all the highvoltage supplies
     was energized and tested up to 10 KV r.m.s., and found to be
     corona free.  The discharge detection system is capable of
     detecting charges of 0.1 pico coulomb.
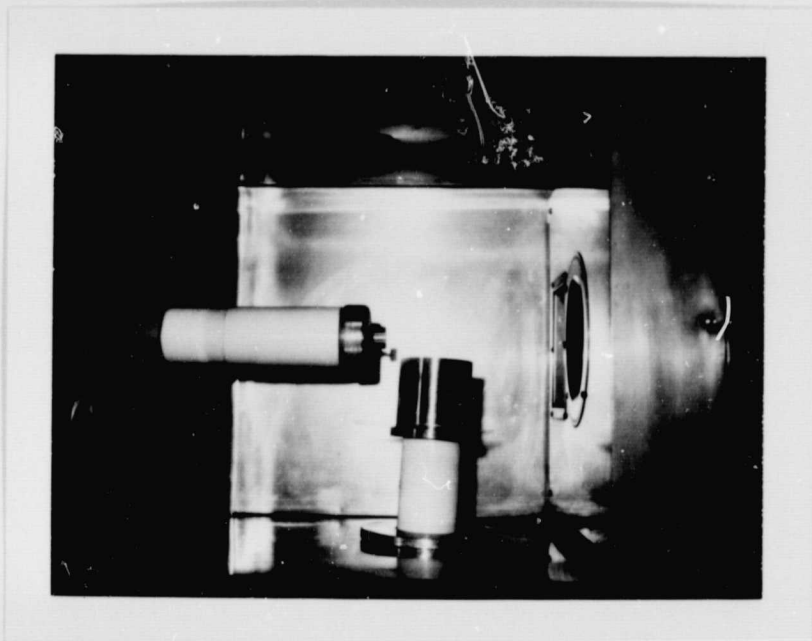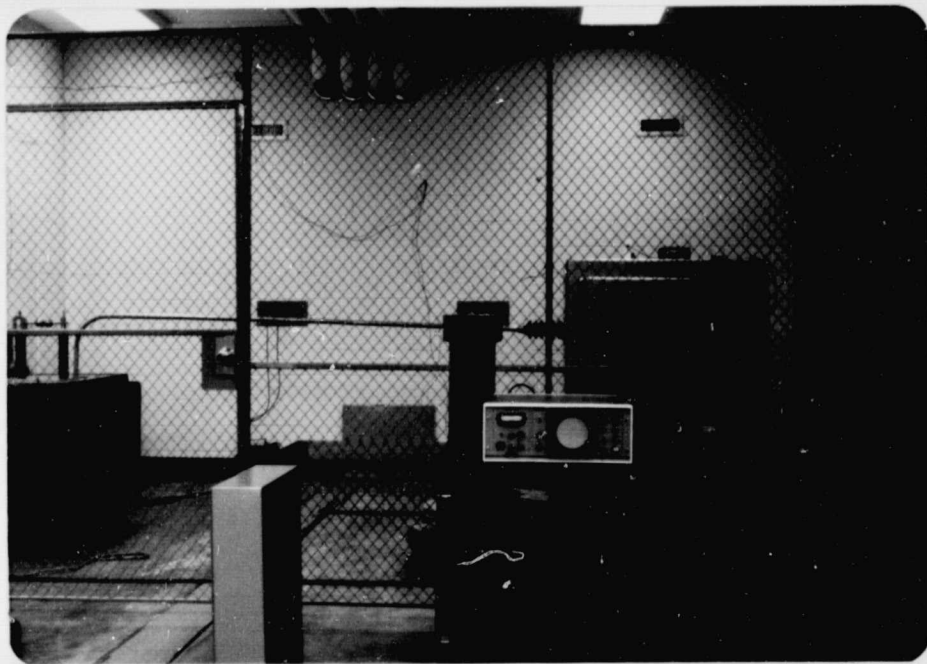
7.   Figs (13) and (14) show the test set up.

Fig 13.



Fig 14          COMPLETE TEST SET UP FOR HIGH VOLTAGE MEASUREMENTS

# MEASUREMENT OF VOLUME RESISTANCE

The volume resistivity of the insulating material will change due to two primary causes:

(1) The Heat generated in the material due to leakage currents which may bring about changes in molecular structure. The insulating material may also deteriorate due to external heat sources, mainly from the solar radiation.

(2) The penetration of electrons and ions, present in the plasma, under the influence of high electric fields.

The principle of measurement of volume resistance consists in measuring the current through the specimen and the Voltage across the specimen.

The unknown Resistance $R_x = V_x/I_x$.

However, the measurements must be made keeping in view the following aspects:

(1) Fringing of the lines of current at the guarded electrode edges may effectively increase the electrode dimensions.

(2)    Because the insulation resistance of solid dielectric specimens
       maybe extremely high, unless extreme case is taken with the
       insulation of the measuring circuit, the values obtained maybe
       more a measure of apparatus limitation than the material itself.

(3)    Where the test specimen has appreciable capacitance, short
       time transients as well as relatively longtime drifts in
       the applied voltage may cause spurious capactive charge an
       discharge currents, which can affect the accuracy of
       measurement.

(4)    When capacitance is very large, the resistance $R_x$ should by
       measured by "Voltage Rate of Change Method" as defined in
       ASTM Standard D257.

(5)    If the plane electrodes are not parallel the current density
       in the specimen will not be uniform and an error may result.
       This error is usually small and maybe ignored.

       Correction to Edge effects and fringing must be applied. [18]

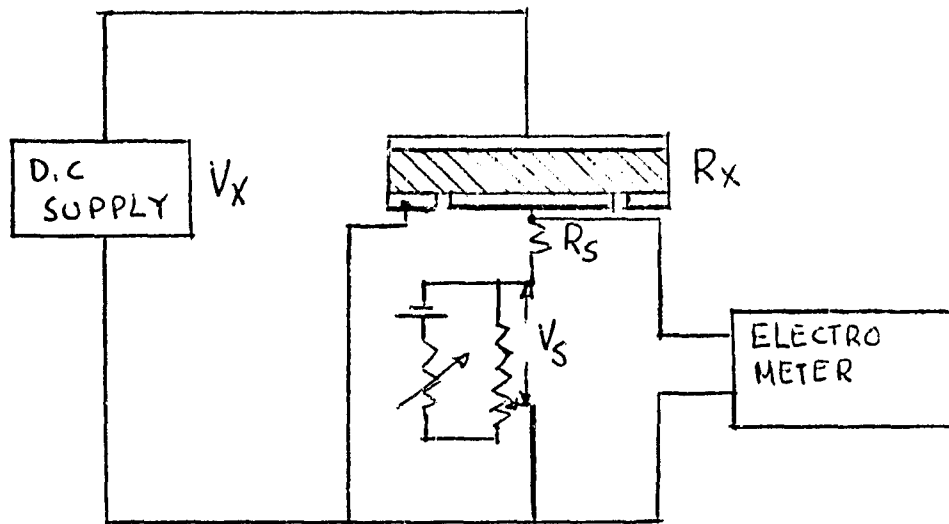Figure (15) shows a circuit for measuring the volume resistance.



Figure (15)

ELECTROMETER AMPLIFIER IS USED AS A VERY SENSITIVE NULL DETECTOR.

At Null $\quad R_x = \dfrac{V_x}{V_S} \cdot R_s$

Where $R_s$ is a Standard resistance.

# MEASUREMENT OF SURFACE RESISTANCE

The surface resistance of the insulating material will change due to the action of changed particles, Plasma and surface arcing. Chemicals and gases in the environment in which the insulating material is located will also alter the chemical and molecular structure of the surface of the insulating material, these by damaging the insulating properties. Figure 16 shows the circuit diagram of the set up used for measuring the surface resistance. In case of insulating materials used on solar cells, only the effects of plasma interaction and thermal effects are of importance in surface degradation.
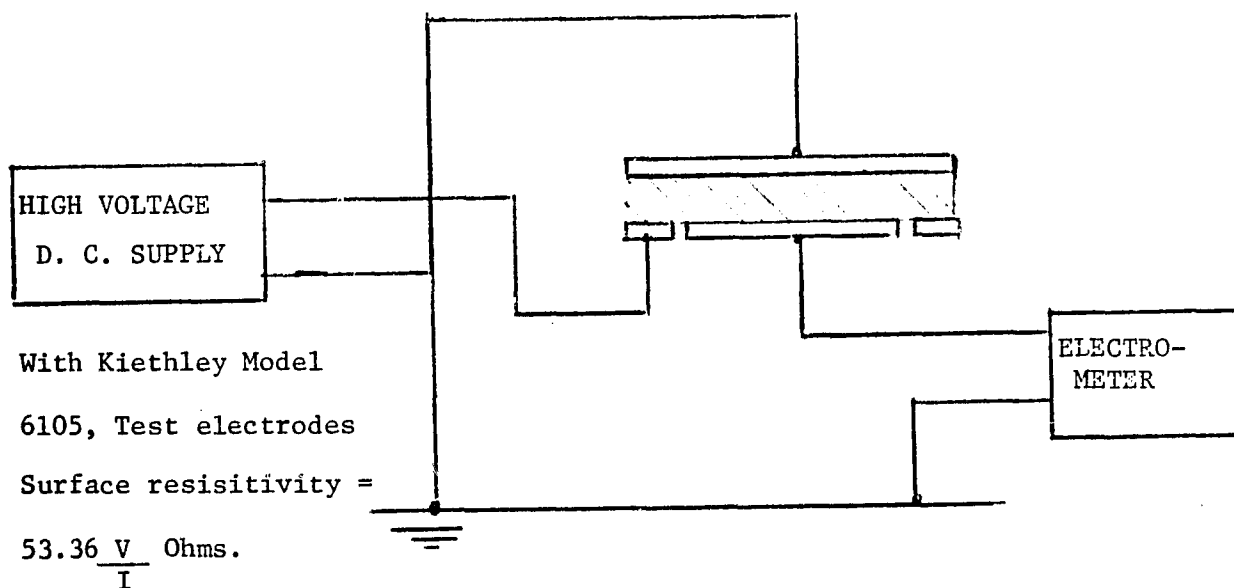


HIGH VOLTAGE
D. C. SUPPLY

With Kiethley Model
6105, Test electrodes
Surface resisitivity =
$53.36 \dfrac{V}{I}$ Ohms.

ELECTRO-
METER

Fig. 17

On thick samples of materials high voltage low current dry arc test according to ASTM Standard D495 is recommended.

## REFERENCES

1.  Evelyn Anagnostu, A.E. Spakowski, "Effects of Electrons, Protons and Ultraviolet Radiation on Plastic Materials". IEEE Photovoltaic SP CON 1974 pp 226-228. NASA Lewis Res.

2.  Arndt, R. A. "Effects of Simultaneous Ultraviolet, Electron and Proton irradiation of Solar Cells" IEEE Photovoltaic SP CON 1975, pp 217-219.

3.  John R. Barton, "Electron and Proton Degradation of Commercially available Solar Cell/Cover Slide Components" IEEE Ph. Vol SP CON 1976, pp 247-249 - BOEING.

4.  S. E. DeForest "Space Craft Charging at Synchronous Orbit" J. Geophysical Research. Vol 77 pp 651-659. 1972.

5.  Stanley Dommitz, N. T. Grier, "The interaction of Space High Voltage Power Systems with Space Plasma Environment". NASA TMX 71554. LEWIS. IEEE Power Electronics Specialists CONFERENCE 1974.

6.  K. L. Kennrud "High Voltage Solar Array Experiments" NASA Report CR 121280 - 1974 - LEWIS/BOEING.

7.  N. John Stevens "Solar Array Experiments on the Sphinx Sattelite" NASA LEWIS TMX 71458 - 1973.

8.  A. Smith, F. Betz, F. Hornbuckle, "Evaluation of Flight Acceptance Thermal Testing for ATS - 6 Solar Array" IEEE Pho Vol SP CON 1975 pp 120-125.

9.  F. C. Treble, A. Dunnet, R. L. Crabb "Comparative Deep Thermal Cycling of Solar Cell Panels" IEEE Ph Vol SP CON 1975 pp 143-152.

10. A. Meulenberg "Radiation Damage to Comsar Non Reflective Cell" IEEE Ph Vol SP CON 1975 pp 204-208.

11. T. J. Faith "Temperature Dependence on Damage Coefficients in Electron Irradiated Solar Cells" IEEE Trans on Nuclear Science 1973 pp 234-237.

12.  J. Bernard, S. Mottet, R. L. Crabb "Photon Degradation of E'ectron and Photon Irradiated Silicon Solar Cells" IEEE Ph Vol SP CON 1976 pp 262-269.

13.  W. Ley, "DFVLR Facility for Thermal Cycling Tests on Solar Panel Samples Under Vacuum Conditions" IEEE Ph Vol SP CON 1976 pp 406-412.

14.  ARNDT, R. A. "Effects of Radiation on Violet Solar Cell" Comsat Rev 1974 pp 41-52.

15.  ASTM, American Standard Methods of Test for A.C. loss Characteristics and Dielectric Constant of Solid Electric insulating materials. Designation D-150 (1970).

16.  Nelson, R. J. Bridge measurements of very low dielectric loss at low temperatures.  Proc. IEEE Vol 121, No. 7 (1974).

17.  Scott, H. and Harris, P. Residual losses in a guard ring micro-electrode holder for solid disk dielectric specimens (1961).

18.  Lauritzen, J. I. "The Effective area of a Grounded Electrode" Annual report, Conference on Electrical Insulation.  NAS - NRC Publication 1141, 1963.

19.  Hartshorn, L and Ward W. H. "The measurement of Permitivity and Power Factor of Dielectrics at frequencies from $10^4$ to $10^8$ cycles per Second". Proc. IEE (London) Vol 79, 1936 pp 597-609.